
In-Flight Load Testing of Advanced Shuttle Thermal Protection Systems

Bianca M. Trujillo, Robert R. Meyer, Jr., and Paul M. Sawko

December 1983

In-Flight Load Testing of Advanced Shuttle Thermal Protection Systems

Bianca M. Trujillo and Robert R. Meyer, Jr.

NASA Ames Research Center, Dryden Flight Research Facility, Edwards, California 93523

Paul M. Sawko

NASA Ames Research Center, Moffett Field, California 94035

1983



National Aeronautics and
Space Administration

Ames Research Center

Dryden Flight Research Facility
Edwards, California 93523

IN-FLIGHT LOAD TESTING OF ADVANCED THERMAL PROTECTION SYSTEMS

Bianca M. Trujillo* and Robert R. Meyer, Jr.*
NASA Ames Research Center, Dryden Flight Research Facility, Edwards, California

Paul M. Sawko[†]
NASA Ames Research Center, Moffett Field, California

Abstract

NASA Ames Research Center has conducted in-flight airload testing of some advanced thermal protection systems (TPS) at the Dryden Flight Research Center. The two flexible TPS materials tested, felt reusable surface insulation (FRSI) and advanced flexible reusable surface insulation (AFRSI), are currently certified for use on the Shuttle orbiter. The objectives of the flight tests were to evaluate the performance of FRSI and AFRSI at simulated launch airloads and to provide a data base for future advanced TPS flight tests. Five TPS configurations were evaluated in a flow field which was representative of relatively flat areas without secondary flows. The TPS materials were placed on a fin, the Flight Test Fixture (FTF), that is attached to the underside of the fuselage of an F-104 aircraft. This paper describes the test approach and techniques used and presents the results of the advanced TPS flight test. There were no failures noted during post-flight inspections of the TPS materials which were exposed to airloads 40% higher than the design launch airloads.

Nomenclature

AFRSI	advanced flexible reusable surface insulation
C _p	pressure coefficient
ENS	elliptical noseshape
FRSI	felt reusable surface insulation
FTF	Flight-Test Fixture
H _p	geopotential altitude
IML	inner mold line
LL	left lower
LM	left middle
LU	left upper
M	Mach number
OML	outer mold line
q	dynamic pressure
RM	right middle

*Aerospace Engineer.

[†]Research Scientist.

This paper is declared a work of the U.S. Government and therefore is in the public domain.

RTV	room-temperature vulcanizing
TPS	thermal protection system
x/c	ratio of distance from leading edge to total length of the FTF location
α	angle of attack
β	angle of sideslip

Introduction

Thermal protection of the Space Shuttle orbiter's substructure is extremely important during reentry. A suitable thermal protection system (TPS) must be a good insulator, light in weight, durable, reusable, and capable of withstanding airloads during launch and entry. The ceramic tiles that make up most of the currently used TPS are costly and time consuming to install or replace, a result of shaping and sizing the individual tiles and of the method of installation. Although the tiles have provided effective thermal protection for the Shuttle, new materials are being developed that promise, among other improvements, reduced complexity of manufacture and installation. Flexible reusable surface insulation (FRSI) and advanced flexible reusable surface insulation (AFRSI) are two TPS materials that are already certified for replacement of some of the white ceramic tiles on the Shuttle. FRSI is a needled felt top-coated with white silicone; AFRSI is a silica-felted batting sandwiched between fabric coverings of silica and glass. The outer material, outer mold line (OML), is the silica fabric and the inner material, inner mold line (IML), is the glass fabric. The layers are sewn together with Teflon-sized silica thread in a 1-in. square stitch pattern. Both materials are described in detail in Ref. 1. The flexible quality of these materials allows larger pieces, like small blankets, to be applied directly to the surface without the strain isolation pad that is presently used with the ceramic tiles.

Previously performed airload tests on these new materials were conducted in wind-tunnel facilities to provide data at specific conditions representative of those encountered during a Shuttle launch. However, the facilities were unable to simulate the entire launch profile because it requires varying conditions over a short period of time that are very difficult to produce in a wind tunnel. In addition, the high dynamic pressures were difficult to achieve in the wind tunnel. In response to these problems, a flight-test program was conducted by NASA Ames Research Center at the Dryden Flight Research Facility on the F-104 Flight Test Fixture.² This aircraft can simulate airload launch profiles, as well as expose test articles to 1.4 times the dynamic pressure experienced during launch. The simulated launch profiles, however, were at a time rate approximately 10 times slower

than the launch rate. Similar airload tests were conducted on the Shuttle tiles prior to STS-1 and are described in Ref. 3.

The FTF was fitted with an elliptical-shaped nose designed to produce a shock (large pressure gradient) at the location of the test articles. This enabled the test articles to be subjected to airloads representative of those experienced on essentially flat areas of the Shuttle during a launch. Some test articles were heated to reentry temperatures and then cooled before the flight tests to determine the effects of high temperatures on the durability of AFRSI.

The objectives of the test program were to evaluate the performance of FRSI and AFRSI, at simulated launch airloads and to provide a data base for comparison with future flight testing of advanced ceramic materials. Most test articles were exposed to two launch profiles, design dynamic pressure ($600\text{--}800\text{ lb/ft}^2$) and 40% above design dynamic pressure ($850\text{--}1140\text{ lb/ft}^2$). The Mach number range was 0.8-1.4 for all profiles. The airloads were documented via pressure measurements, and the test articles were subjectively examined in preflight and postflight visual inspections. The tests were essentially limited to airloads and did not include the effects of the booster orbiter's vibro-acoustic environment or simultaneous aero/thermal loads.

Description of Test Facility

F-104 Aircraft

A specially equipped F-104 aircraft was used as a carrier vehicle for these tests. The aircraft is instrumented with special cockpit displays that provided the unique capability of precisely flying the required launch profiles; furthermore, it was modified to accept a lower fuselage fin, the FTF, on which the test articles were installed. The FTF was modified to create a flow field representative of many areas on the orbiter within a large Mach-number/dynamic-pressure envelope. Reference 2 describes the facility and its capabilities and Fig. 1 shows the fin mounted on the aircraft.

Flight Test Fixture

A nose having an elliptical cross section and made of foam and fiberglass was fitted to the Flight Test Fixture. Attached to the FTF, the nose created a 1.5 in. aft-facing step with respect to the original sides of the FTF. This step allowed test articles of thicknesses up to 1.5 in. to be installed on the sides of the FTF, behind the nose. Fiberglass panels, 1.5 in. thick, were installed behind the test articles. Side and top views of the FTF showing the nose, test articles, and fiberglass panels are presented in Fig. 2. A photograph of an AFRSI test article mounted on the FTF is shown in Fig. 3.

The FTF was equipped with an instrumentation system, including a nose boom which was separate from the aircraft air-data system. The FTF surface pressures were measured by a 48-port, mechanical, pressure scanning transducer; two 32-port, electronically scanned, multiple pressure transducer assemblies; and two individual transducers. Air-data parameters measured from airspeed transducers,

such as Mach number and dynamic pressure, were determined from both the aircraft and FTF nose booms. Chord and spanwise surface pressures were obtained from the 62 orifice locations shown in Fig. 4.

Description of Flexible Insulation Construction

Three flexible thermal protection systems were tested in this flight-test program. These consisted of felt reusable surface insulation (FRSI) and two types of advanced flexible reusable surface insulation (AFRSI). These thermal protection systems could be fabricated in variable thicknesses and in large blanket-like pieces. FRSI is a certified, flexible felt system made of an aromatic polyimide, needled felt, which had been heat treated, then top-coated with a white silicone, room-temperature vulcanizing coating.

One of the two AFRSI blankets flight tested was an experimental version of the AFRSI designated as "in-house" AFRSI that had been evaluated in screening studies from wind-tunnel testing. This in-house AFRSI is constructed as shown in Fig. 5. The outer mold line (OML) silica fabric consisted of a silica style 593, in a 5H satin-weave pattern with a standard aminosilane finish. This construction yields a fabric that weighs 7.0 oz/yd^2 and is 0.010 in. thick. The inner mold line (IML) fabric was a silica style 503 fabric in a plain-weave pattern with the standard aminosilane finish. The fabric weighs 3.3 oz/yd^2 and is 0.005 in. thick. Sandwiched between these two fabrics is a 0.5-in.-thick layer of silica felt or batting in a 6-lb/ft^3 nominal density. The blanket is held together by 0.017-in.-diam Teflon-sized silica sewing thread in a 1-in. stitch pattern using a standard 301 lock stitch.

The second type of AFRSI, referred to as baseline AFRSI, was the principal TPS tested in this study. Baseline AFRSI was fabricated and prepared according to Shuttle specifications.⁴ The general construction is also similar to that shown in Fig. 5. The OML was a silica style 570 fabric with a 5H satin weave and with the standard aminosilane finish. The fabric weighs 19.5 oz/yd^2 and is 0.027 in. thick. The IML fabric used was a glass cloth. A 6-lb/ft^3 silica felt or batting in a 0.5 or 1 in. thickness was sandwiched between these two fabrics. The blanket was held together by an OML Teflon-sized silica thread (0.020 in. diam) and an IML glass sewing thread in a 1-in. stitch pattern, using a modified lock stitch which moves the loop to the bottom of the IML fabric surface.

FRSI and baseline AFRSI are of the same quality and construction currently used on the Space Shuttle Challenger. The baseline AFRSI, as received for assembly into the test article, had been fabricated, heat cleaned, and waterproofed according to Shuttle specifications; the in-house AFRSI was not. The condition of the baseline AFRSI blankets as tested (i.e., in respect to loose or broken threads and puckering) were representative of what is currently accepted for use on the orbiter.

Description of the Flight AFRSI Test Articles

The flight test covered the five configurations listed in Table 1. The test article had either butt-joint or one-piece flat configurations, as shown in Fig. 6. Each test article blanket was bonded to an aluminum plate contained within an unfinished wood frame. To protect the unfinished material edges near the wood frame, an aluminum frame overlay was placed over the edges of the test material, exposing approximately a 26-in. by 15.5-in. area of the blanket. A schematic of a test article is presented in Fig. 7.

Standard room-temperature vulcanizing (RTV) adhesive was used to bond the test material and was also used on the orbiter. The vacuum bag bonding technique, the standard bonding technique used for the Shuttle,⁵ was used for test articles containing multiple butt-jointed configurations (configurations 3 and 4), and the weight-pressure technique was used for one-piece flat configurations (configurations 1-5).

The FRSI test article (configuration 1) was not instrumented with pressure orifices. The AFRSI test articles located on the right side of the FTF (configurations 3-5) were instrumented with only one row of subsurface pressure orifices along the center of the test article (Fig. 4). The AFRSI test articles located on the left side of the FTF were instrumented with three rows of pressure orifices, two flush rows and one subsurface row, located in the middle of the test article (configurations 2-5), also shown in Fig. 4. Before bonding, the subsurface orifice holes were drilled, and pressure tubes were mounted through the aluminum substructure so that they would come in contact with the IML. The area around the pressure-tube holes was kept free of the RTV to prevent blockage. The remaining frame pressure orifices were installed after the bonding process.

Test Approach and Procedures

Airload testing of the test articles required the tailoring of the flow field to simulate Shuttle conditions over the FTF. Therefore, an elliptically shaped nose was designed to produce a shock (large pressure gradient) at the location of the test article. The design pressure distribution is shown in Fig. 8. The dynamic-pressure/Mach-number curves shown in Fig. 9 represent the simulated launch profiles that were used in this study. As shown, the design and 1.4 design launch profiles covered a dynamic pressure range from 800 to 1140 lb/ft². The Mach number range is the same for all launch profiles.

It was extremely important that the required flight conditions be maintained; this was accomplished by using a flight trajectory guidance system referred to as the uplink guidance system. The uplink guidance system uses an analog cockpit display that indicates deviations from the desired flight conditions in real time; it is discussed in detail in Ref. 6. One parameter displayed on the uplink guidance system was sideslip (β). The sideslip values were obtained by comparing the measured static pressure values of orifices L16 and R7 (Fig. 4); their differences were displayed on the uplink system.

The first flights in the test program were calibration flights using configuration 1. The objectives of these flights were to document the pressure distribution of the FTF with the elliptically shaped nose and to expose FRSI to the airloads environment of the FTF. The left side of the FTF was fitted with a fiberglass side panel without a test article. This made the left side of the FTF one continuous section containing all flush orifices for detailed pressure measurements. The orifice locations are shown in Fig. 4. The right side of configuration 1 contained the FRSI test article. Because similar material had survived the airloads of previous Shuttle launches, it was felt that exposure of FRSI to the FTF flow environment would to some degree validate the test method of using the FTF for airload tests.

In-house AFRSI, configuration 2, had been extensively tested for airloads in wind-tunnel tests and was flight tested to establish a comparison between the results obtained by wind-tunnel-imposed airloads and in-flight FTF airloads.

The remaining configurations (3-5) were the baseline AFRSI material. This was the principal TPS to be tested. It was flight tested to evaluate the type of material currently used on the Shuttle, as well as to establish a data base for future flight testing.

Analysis of the performance of the test articles was subjective and consisted of preflight and postflight inspections. Airloads were measured via pressure distribution data obtained during each flight. Figure 10 presents two examples of the pressure-distribution data for the middle row of orifices on the right and left test articles for the same flights and test conditions. The two pressure distributions are essentially the same, showing that symmetrical flow existed and that the right and left test articles were exposed to the same flow field.

Each design profile required a separate flight which was completed in about 30 min. For takeoff and climb to initial conditions, as well as descent after completion of the profile and landing, the aircraft was restricted to an airspeed of 300 knots to insure that any damage incurred was due solely to airloads experienced during the simulated launch profile.

The test article samples for configurations 4 and 5 were thermally cycled in a heat facility to representative reentry temperatures. The objective of the heat testing was to determine if there were any detrimental effects of previous exposure to elevated temperature on the ability of the baseline AFRSI materials to withstand airloads. Figure 11 shows the surface temperature versus time for one cycle of the heating test. As shown in Fig. 11, the surface of the TPS was heated to 1200°F for three 10-min cycles, or a total of 30 min.

Test Results and Discussion

Typical results of simulated Shuttle launch airload flight tests performed on the advanced TPS are presented in Table 2. They are considered representative of areas that are relatively flat and for which no secondary flows are involved

(i.e., separated flow or vortex impingement). The tests were not intended to simulate areas of curvature such as the OMS pods (where a failure occurred on STS-6).

Pressure Distribution Data

A series of pressure distributions obtained from the side panel of configuration 1 is presented in Fig. 12; the figure shows that the desired pressure distribution was obtained. A large pressure gradient was generated over the test article and moved aft with increasing Mach number. The data presented in Fig. 12 are for the 1.0 design profile, but it is representative of all three launch profiles as well.

Figure 13 presents the chordwise pressure distributions obtained from configuration 1 (fiberglass side panel) and from configuration 3 (AFRSI test article). The pressure distributions presented for both configurations are from the center row of orifices during a 1.4 design profile at a Mach number of 1.15. The two pressure distributions differ significantly. However, the configuration 3 orifices are subsurface, below the AFRSI blanket. The subsurface pressure measurements were expected to be equivalent to the surface pressures, but they were not. It appears that the material attenuates the pressure between the OML and the IML. The large pressure gradient over the test article may cause the more positive pressure at the aft end of the test article to feed forward along the IML, resulting in a higher subsurface pressure. However, having both flush and subsurface pressure measurements is beneficial, since they provide an estimate of the pressure loads between the two surfaces of the TPS.

The results of a final analysis performed on the pressure distribution data are presented in Fig. 14. Shown are chordwise pressure distributions for each design profile at the same flight conditions. The pressure distributions are basically the same in shape, as well as in magnitude, for all three profiles. The slightly more positive pressure distribution for the 1.0 design case was a result of the aircraft flying at a higher trim angle of attack (α) to maintain the test conditions.

FRSI

FRSI configurations 1 and 2 were tested and showed no degradation. Based on these results it was decided to test the remaining AFRSI articles at the 1.0 and 1.4 design profiles only and to eliminate the 0.5 design profile.

AFRSI

In-house AFRSI, configuration 2, provided flight data to be compared with data from the wind-tunnel tests. No significant differences in the performance of the material were noted, and, as presented in Table 2, no failures occurred.

The baseline AFRSI test articles (configurations 3-5) contained loose or broken threads and areas of slight puckering, especially the butt-jointed configurations (configurations 3 and 4), which were noted during preflight inspections. An example of this is shown in Fig. 15. These conditions were not aggravated, however, even when the materials were tested at 40% above the design

airloads. The one exception (configuration 3) manifested itself as an increase in puckering at the joint running perpendicular to the flow. This increased puckering created a small step in the test article, but no thread damage. All the test articles were judged acceptable for further testing after postflight inspections.

Conclusions

The flight-test approach used in this study was to evaluate the performance of advanced TPS at simulated airloads typical in magnitude of those observed on the Shuttle during launch. Using the FTF as a test facility provided data that are representative of relatively flat surfaces. In general, this approach was expedient and effective because of 1) the large dynamic-pressure/Mach-number envelope of the carrier aircraft and 2) the ability to expose full-scale articles to realistic airloads.

The surface-pressure data obtained from the side panel of configuration 1 confirmed that the desired pressure distribution was obtained. The FRSI test article, configurations 1 and 2, aided in confirming the test technique, since it had performed successfully on previous Shuttle missions.

No failures were observed on the AFRSI test articles that were subjected to launch airloads that were 40% above design. The butt-jointed articles (configurations 3 and 4) contained loose or broken threads and puckering which were not adversely affected by the airload testing. Heat testing performed before flight testing (configurations 4 and 5) produced no detrimental effects on the ability of the AFRSI materials to withstand airloads.

The AFRSI failure that occurred on the OMS pods during the STS-6 mission was in an area of curvature; it may also have been an area in which separated flow or secondary flow impingement occurred. Therefore, the results of this study are not directly applicable to STS-6 since these flow types were not simulated.

References

- ¹Goldstein, H., Leiser, D., Larson, H., and Sawko, P. M., "Improved Thermal Protection System for the Space Shuttle Orbiter," AIAA Paper 82-0630-Cp, May 1982.
- ²Meyer, R. R., Jr., "A Unique Flight Test Facility: Description and Results," ICAS Paper 82-5.3.3, Aug. 1982.
- ³Meyer, R. R., Jr., Jarvis, C. R., and Barnburg, J., "In-Flight Aerodynamic Load Testing of the Shuttle Thermal Protection System," AIAA Paper 81-2468, Nov. 1981.
- ⁴Thatcher, U. S. and McGuire, M. B., "Fabrication of Flexible Insulation - Space Shuttle Orbiter," MA0605-315, Rockwell International, Downey, Calif., 1981.

⁵Thomas, D. and McGuire, M. B., "RTV Silicone Adhesive-Bonded Flexible Insulation Blanket-Space Shuttle Orbiter," MA0606-317, Rockwell International, Downey, Calif., 1981.

⁶Meyer, Robert R., Jr. and Schneider, Edward T., "Real-Time Pilot Guidance for Improved Flight Test Maneuvers," AIAA Paper 83-2747, Nov. 1983.

Table 1 F-104 advanced TPS tests: flight configurations and summary

Configuration	Left test article	Right test article	Profile design
1	Fiberglass panel	FRSI	0.5, 1.0, 1.4
2	In-house AFRSI; nominal 0.5 in. thick, no thermal cycling	FRSI	1.0, 1.4
3	Baseline AFRSI; 0.5 in. thick, heavy OML, no thermal cycling, butt joint	Same as left except no butt joint	1.0, 1.4
4 ^a	Baseline AFRSI; 1 in. thick, heavy OML, thermal cycling, butt joint	Same as left except no butt joint	1.0, 1.4
5 ^a	Baseline AFRSI; 1.5 in. thick, light OML, thermal cycling	Baseline AFRSI; 1 in. thick, light OML, thermal cycling	1.0, 1.4

^aHeat cleaned and waterproofed.

Table 2 Summary of posttest observations

Config-uration	Profile design	Pretest observations		Postflight observations ^a	
		Left	Right	Left	Right
1	0.5	None	None	NC	NC
	1.0	None	None	NC	NC
	1.4	None	None	NC	NC
2	1.0	None	None	NC	NC
	1.4	None	None	NC	NC
3	1.0	RTV spots,	RTV spots,	NC	NC
	1.4	loose threads	loose threads	Slight step at joint	NC
4	1.0	Loose and	Loose thread,	NC	NC
	1.4	broken threads, slight step at joint in parallel direction	RTV spot	NC	NC
5	1.0	Slight pucker	Tight thread	NC	NC
	1.4	at top, tight threads		NC	NC

^aNC = no change.

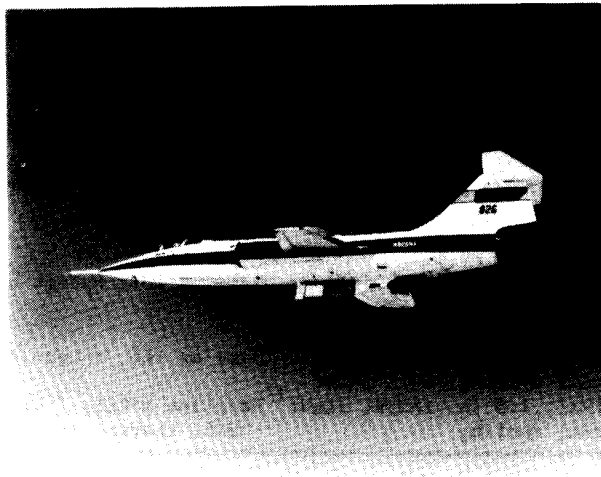


Fig. 1 F-104 in flight with Flight Test Fixture mounted on the underside of the fuselage.

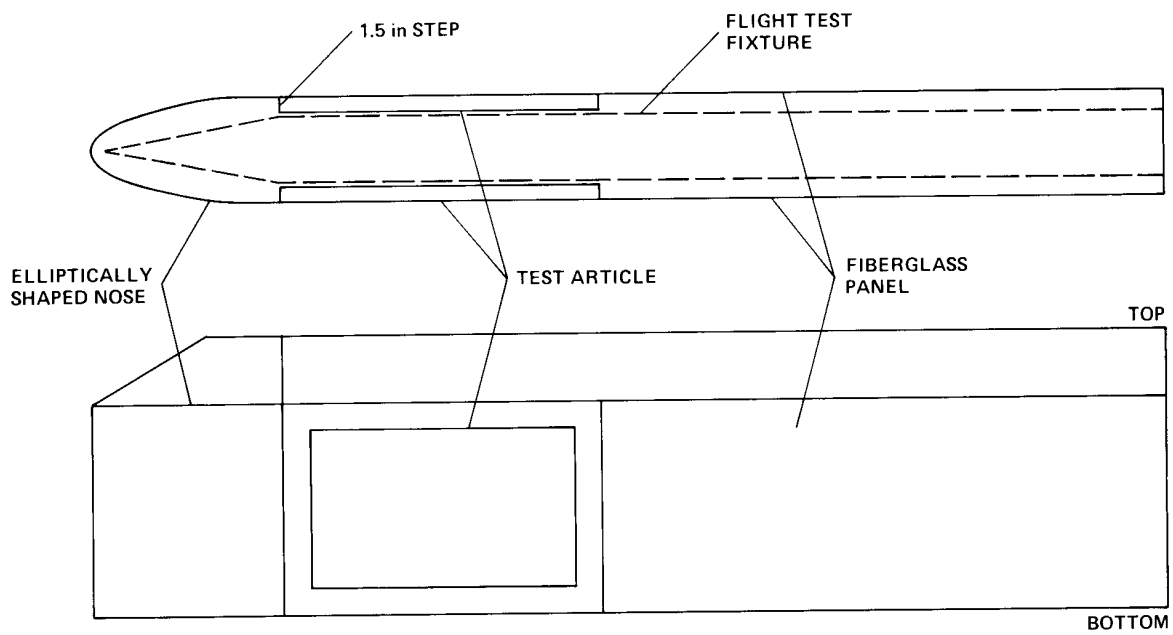


Fig. 2 Top and side view of the FTF with the locations of the elliptically shaped nose, test articles, and side panels.

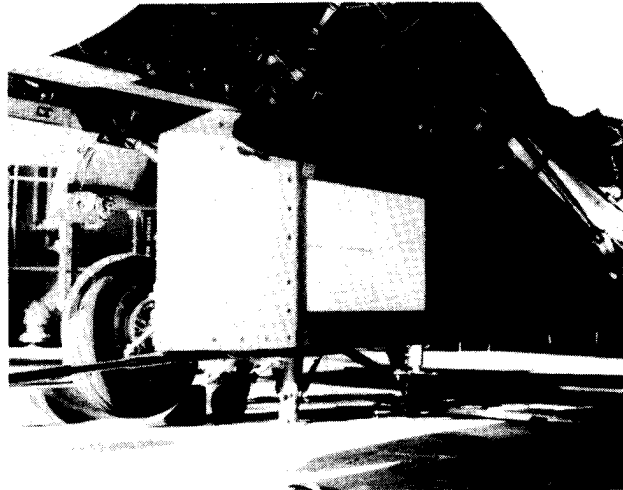


Fig. 3 Butt-joint configuration mounted on the FTF behind the elliptically shaped nose.

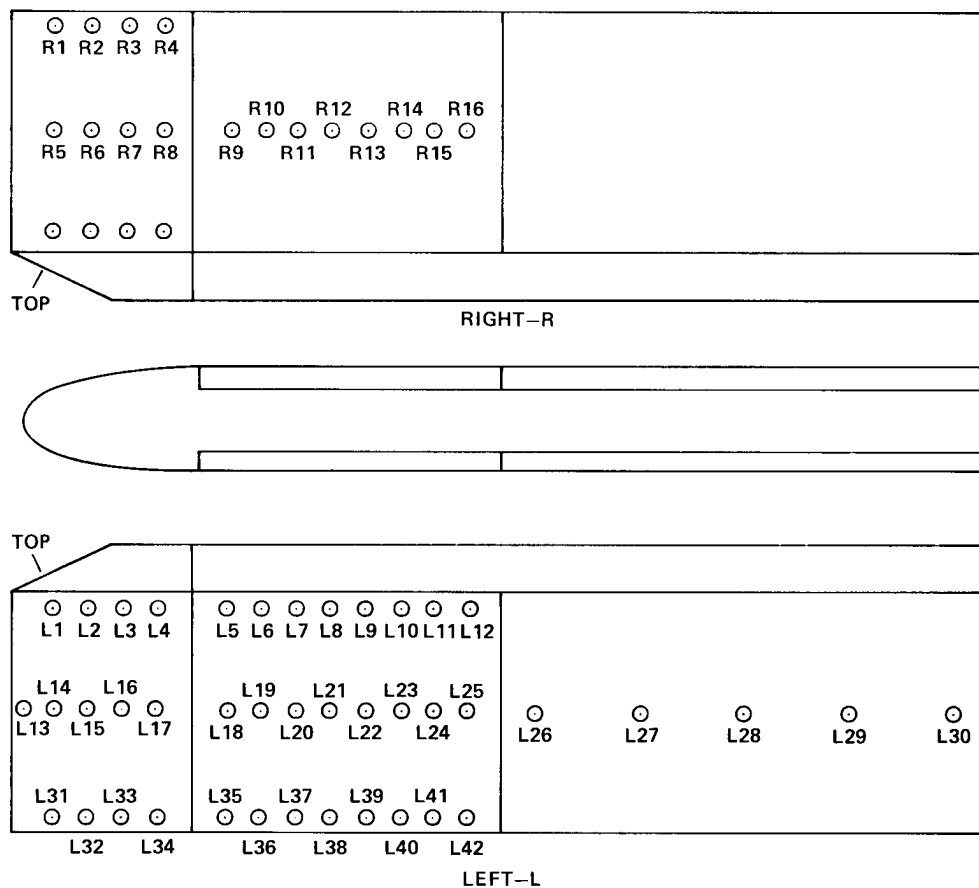


Fig. 4 Top foldout view of the FTF showing locations of pressure orifices.

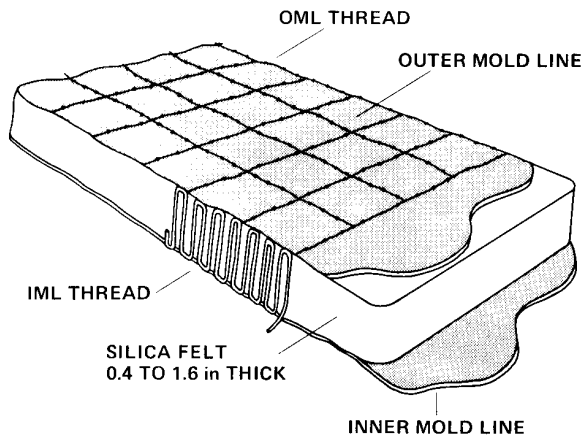


Fig. 5 Construction of advanced flexible reusable surface insulation (AFRSI).

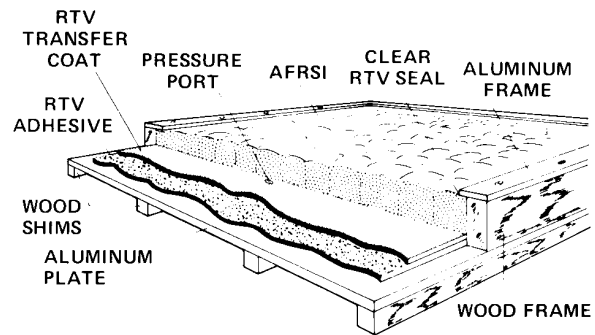
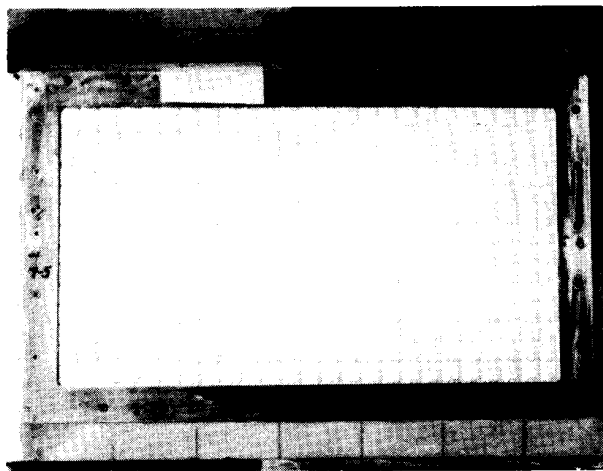
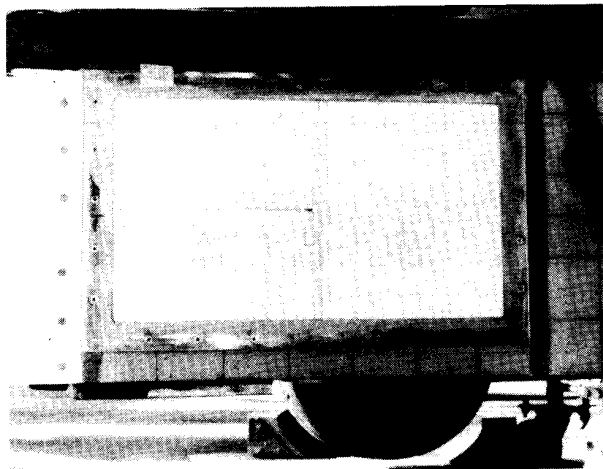


Fig. 7 AFRSI test article.



a) One-piece flat.



b) Butt joint.

Fig. 6 Configuration of typical test articles.

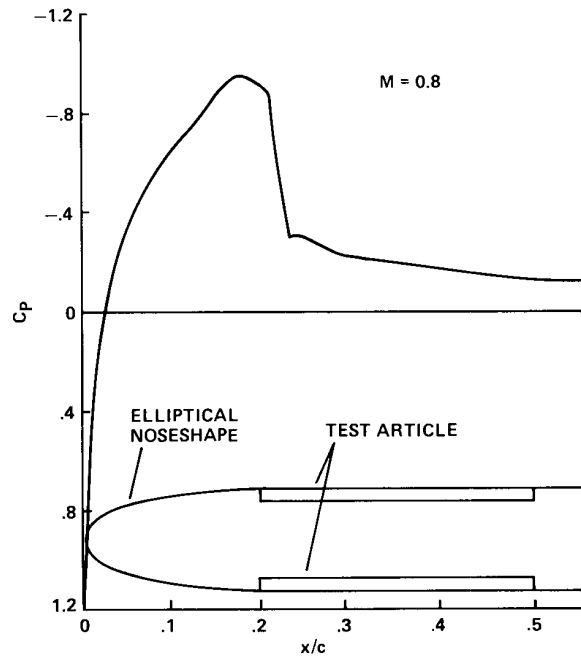


Fig. 8 Theoretical pressure distribution on test surface with elliptically shaped nose.

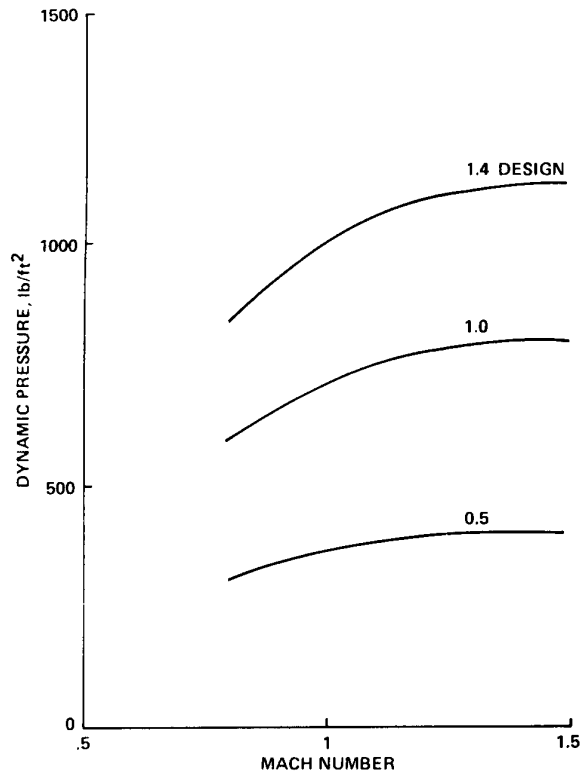


Fig. 9 Variation of dynamic pressure as a function of Mach number for three Shuttle launch profiles.

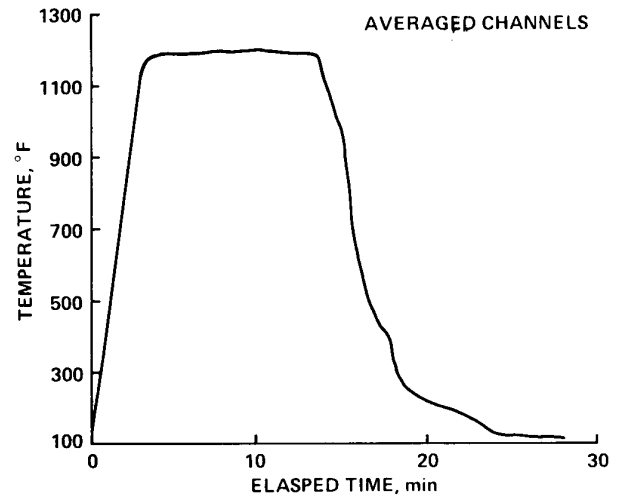


Fig. 11 Variation of AFRSI surface temperature during one heating and cooling cycle.

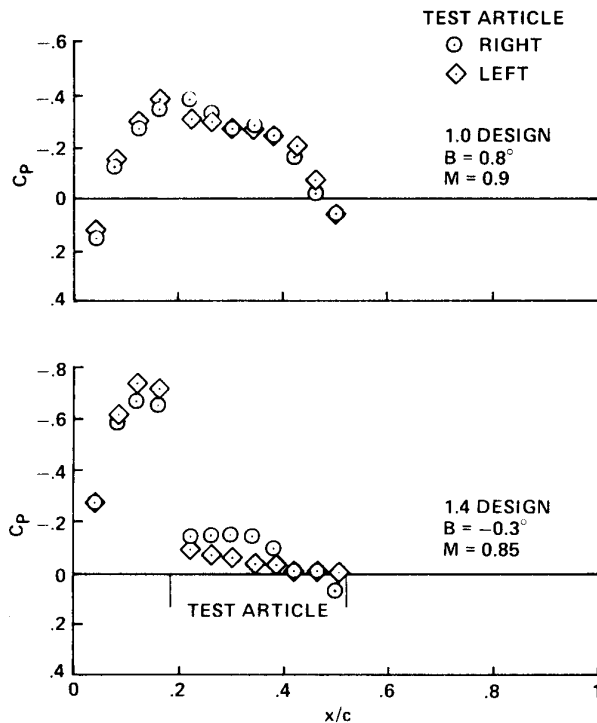


Fig. 10 A comparison of the pressure distribution data for the right and left sides of the FTF at two values of sideslip (β) (middle orifice row).

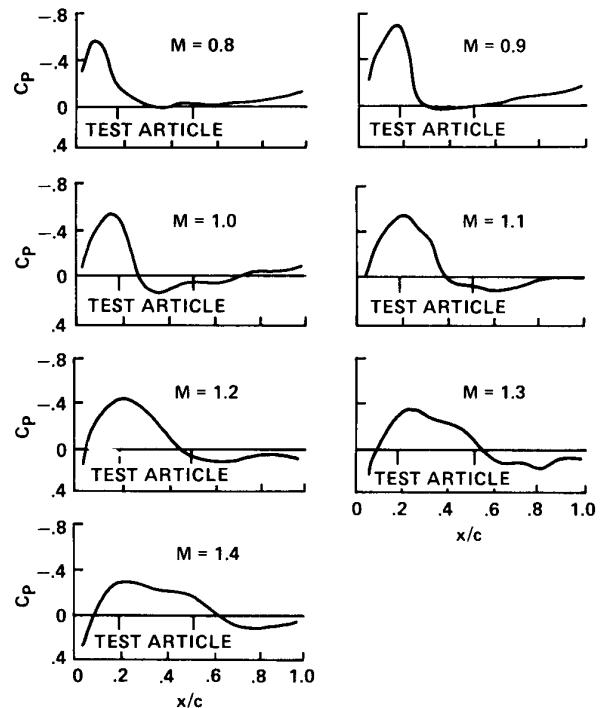


Fig. 12 Series of representative chordwise pressure distributions for a 1.0 design launch profile.

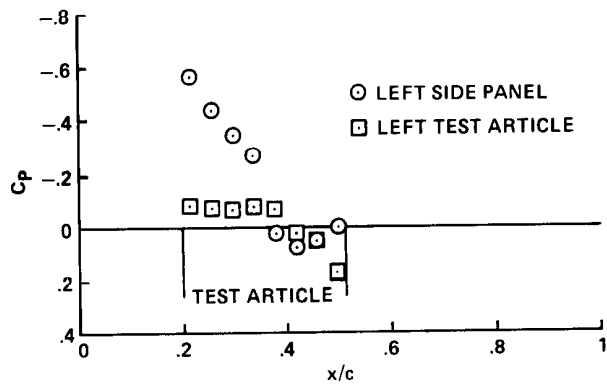


Fig. 13 A comparison of the left side panel and left test article pressure distributions: 1.4 design, $M = 1.15$, $\alpha = 1.6$.

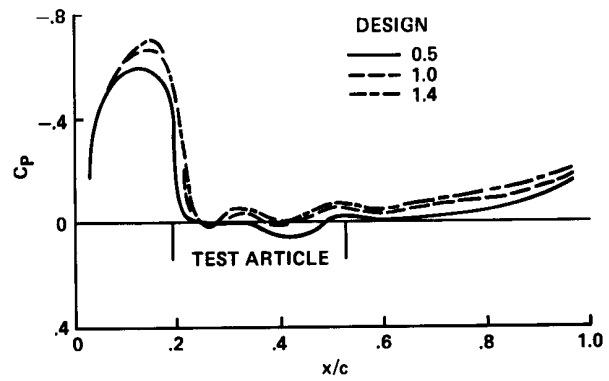


Fig. 14 Comparison of launch profile pressure distributions: 1.4 design, $M = 1.5$, $\alpha = 1.6$.

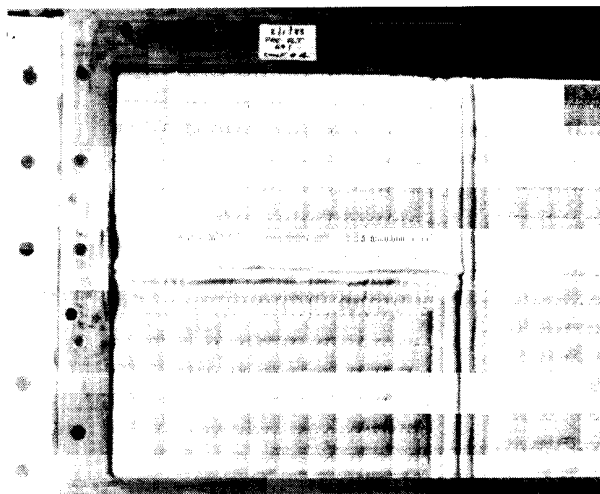


Fig. 15 Example of loose and broken threads and puckering, typical of the baseline AFRSI test blankets.

